Galactosidase-catalyzed fluorescence amplification method (GAFAM): sensitive fluorescent immunohistochemistry using novel fluorogenic β-galactosidase substrates and its application in multiplex immunostaining

（ガラクトシダーゼ触媒蛍光増幅法(GAFAM)：新規の蛍光発生ベータガラクトシダーゼ基質を利用した高感度蛍光免疫組織化学とそのマルチプレックス免疫染色法への応用）

平田　勝啓

Hirata, M., Kogame, T., Adachi, S. et al. Galactosidase-catalyzed fluorescence amplification method (GAFAM): sensitive fluorescent immunohistochemistry using novel fluorogenic β-galactosidase substrates and its application in multiplex immunostaining. Histochem Cell Biol (2022). https://doi.org/10.1007/s00418-022-02162-5

Histochemistry and Cell Biology
https://doi.org/10.1007/s00418-022-02162-5

主論文

ORIGINAL PAPER

Galactosidase-catalyzed fluorescence amplification method (GAFAM): sensitive fluorescent immunohistochemistry using novel fluorogenic β-galactosidase substrates and its application in multiplex immunostaining

Masahiro Hirata[1,3] · **Toshiaki Kogame**[2] · **Souichi Adachi**[3] · **Hironori Haga**[1]

Accepted: 16 October 2022

Abstract
Multiplex immunohistochemistry/multiplex immunofluorescence (mIHC/mIF) enables the simultaneous detection of multiple markers in a single tissue section by visualizing the markers in different colors. Currently, tyramide signal amplification (TSA) is the most commonly used method because it is heat resistant to multiplexing. SPiDER-βGal (6′-(diethylamino)-4′-(fluoromethyl)spiro[isobenzofuran-1(3H),9′-[9H]xanthen]-3′-yl β-D-galactopyranoside), a novel fluorogenic substrate of β-galactosidase (β-gal) was reported recently. Its properties are favorable for application in sensitive mIF based on quinone methide chemistry. Combining SPiDER-βGal with its related substrates, a novel, sensitive fluorescent IHC method for formalin-fixed paraffin-embedded (FFPE) sections was developed, named the galactosidase-catalyzed fluorescence amplification method (GAFAM). Evaluation of GAFAM indicated the following characteristics: (1) the entire GAFAM procedure was complete within a few hours; (2) the optimal working concentration of the substrates was 20 μM; (3) the fluorescent product was heat resistant; (4) the GAFAM exhibited sensitivity comparable with that of TSA, which was higher than that of conventional IF; and (5) the GAFAM was applicable to mIF and multispectral imaging. GAFAM is expected to be applicable to IF (or mIF in combination with TSA), and is a promising tool for facilitating morphological research in various fields of life science.

Keywords Immunohistochemistry · β-Galactosidase · Quinone methide · Tyramide signal amplification (TSA) · Catalyzed reporter deposition (CARD) · Multispectral imaging

Introduction

Immunohistochemistry (IHC) and immunofluorescence (IF) are essential techniques in the life sciences (Eyzaguirre and Haque 2008; Teixidó et al. 2018; Sukswai and Khoury 2019; Cimino-Mathews 2021; Pratapa et al. 2021).

✉ Masahiro Hirata
hiratama@kuhp.kyoto-u.ac.jp

1 Department of Diagnostic Pathology, Kyoto University Hospital, 54 Shogoin-Kawahara-Cho, Sakyo-Ku, Kyoto 6068507, Japan

2 Department of Dermatology, Kyoto University Hospital, Sakyo-Ku, Kyoto 6068507, Japan

3 Department of Human Health Sciences, Graduate School of Medicine, Kyoto University, Sakyo-Ku, Kyoto 6068507, Japan

Multiplex IHC/multiplex IF (mIHC/mIF) allows simultaneous detection of multiple markers (Stack et al. 2014; Tan et al. 2020; Viratham Pulsawatdi et al. 2020). Tyramide signal amplification (TSA), also known as the catalyzed reporter deposition system (CARD), is the most common multiplexing method. TSA involves the activation of the tyramide radical by horseradish peroxidase (HRP) in the presence of hydrogen peroxide to form covalent bonds with aromatic amines such as tyrosine or tryptophan residues in peptide chains, thereby achieving high sensitivity and heat resistance (Bobrow et al. 1989; Speel et al. 1997). However, the TSA method using HRP has the following disadvantages: (1) endogenous peroxidase activity causes nonspecific background signals, (2) background quenching using hydrogen peroxide has detrimental effects on some epitopes, and (3) the antibody denaturation step (mainly heating) inhibits cross-reaction during each multiplex

Published online: 14 November 2022

staining cycle, causing undesired sample damage and loss of the target antigenicity.

β-Galactosidase (β-gal) is a glycoside hydrolase that cleaves the β1,4-linked terminal galactose residues of β-galactosides. This enzyme is extensively used in various reporter systems, including as LacZ-containing plasmids in molecular biology (Price et al. 1987; Mohler and Blau 1996), markers for aged cells with senescence-associated β-gal (SA-β-gal) (Dimri et al. 1995; Sugizaki et al. 2017), and labeling enzymes in enzyme-linked immunosorbent assays (ELISA) and chromogenic IHC (Bondi et al. 1982; van der Loos et al. 1993; van der Loos 2010). β-gal is commonly coupled with chromogenic or fluorogenic substrates (Debacq-Chainiaux et al. 2009).

Recently, 6′-(Diethylamino)-4′-(fluoromethyl) spiro[isobenzofuran-1(3H),9′-[9H]xanthen]-3′-yl β-D-galactopyranoside (SPiDER-βGal), a β-gal substrate that emits yellow fluorescence, was used to detect LacZ-expressing cells (Doura et al. 2016). Additionally, SPiDER-βGal has been used for the SA-β-gal assay (Sugizaki et al. 2017) and intraoperative imaging to detect living cancer cells (Nakamura et al. 2017). The catalytic cascade of SPiDER-βGal generates a highly fluorescent product via the following reactions: (1) hydrolysis of the β-galactosyl group of SPiDER-βGal by β-gal, (2) quinone methide intermediate generation by the loss of fluoride, (3) covalent immobilization of quinone methide on proteins in the proximity of β-gal with nucleophiles (e.g., amine or thiol group), and (4) emission of strong fluorescence owing to the formation of fluorescent rhodol derivatives (Fig. 1a). Other novel fluorogenic β-gal substrates include two coumarin derivatives, 4-methyl-8-fluoromethylumbelliferyl-β-D-7-galactopyranoside (MUGF) and its analog MUGF3 (the detailed structure is proprietary). Their reaction mechanisms are based on quinone methide chemistry, similar to that of SPiDER-βGal. MUGF has recently been reported as a substrate with sensitive fluorogenicity in immunocytochemistry (ICC) for living cells (Noguchi et al. 2020). This ICC was developed as a qualitative method for antigen detection; however, it is not suitable for assessing antigen localization.

Conventional fluorescent probes, such as fluorochrome-conjugated tyramides, constantly emit fluorescent signals, causing high background signals without harsh washout steps. However, activatable substrates such as SPiDER-βGal can circumvent this problem. Additionally, the fluorescence of SPiDER-βGal is expected to have heat resistance derived from covalent bonds, similar to that of TSA, and may be applicable to mIF. Although activatable and covalent-binding substrates for IF on formalin-fixed paraffin-embedded (FFPE) samples have been explored, there is no published literature on the application of β-gal substrates for this purpose.

In this study, a novel, sensitive fluorescent IHC method using fluorogenic β-gal substrates that is applicable to FFPE tissue sections is developed. The principle of this signal amplification system, which is named the galactosidase-catalyzed fluorescence amplification method (GAFAM), is illustrated in Fig. 1b. The method is optimized for mIF and expanded to multispectral imaging.

Materials and methods

Antibodies

The antibodies used in this study are listed in Table 1. All antibodies were diluted using 1% bovine serum albumin (001-000-161; Jackson ImmunoResearch, West Grove, PA, USA) dissolved in Tris-buffered saline (TBS, 50 mM, pH 7.4; Takara Bio, Kyoto, Japan).

Fluorogenic substrates of β-gal and fluorochrome-conjugated tyramides for TSA

SPiDER-βGal (SG02) was purchased from Dojindo Laboratories (Kumamoto, Japan). MUGF and MUGF3 were provided by Dr. Takashi Shimomura (Dojindo Laboratories). The excitation/emission wavelengths of the fluorescent products were determined as follows: 350/450 nm for MUGF, 400/450 nm for MUGF3, and 525/560 nm for SPiDER-βGal (Doura et al. 2016; Noguchi et al. 2020). The β-gal substrates were diluted in phosphate-buffered saline (PBS, 10 mM, pH 7.4) containing 10 mM of $MgCl_2$.

Cy3- and Cy5-conjugated tyramides (Cy3-tyramide, 11065; Cy5-tyramide, 11066) were purchased from AAT Bioquest (Sunnyvale, CA, USA). Other fluorochromes, 7-amino-4-methyl-3-coumarinacetic acid *N*-succinimidyl ester (AMCA, 08450; Sigma-Aldrich, Darmstadt, Germany), 7-(diethylamino) coumarin-3-carboxylic acid *N*-succinimidyl ester (DEAC, D5799; TCI Chemicals, Tokyo, Japan), and 5/6-carboxyfluorescein *N*-succinimidyl ester (fluorescein, 46410; Thermo Fisher, Waltham, MA, USA), were conjugated with tyramide, according to a procedure reported in literature (Hopman et al. 1998; Clutter et al. 2010). Fluorochrome-conjugated tyramides were diluted to 2.5 μM (1:200–1:500, depending on the molecular weight) in PBS containing 0.0015% hydrogen peroxide.

Imaging equipment and software

Sample slides were imaged using a BX63 fluorescence microscope (Olympus, Tokyo, Japan) with a DP80 dual charge-coupled device (CCD) camera (Olympus, 1360 × 1024 pixels) in the 24-bit RGB color or 14-bit grayscale mode. The objective lenses were Uplan Super Apo,

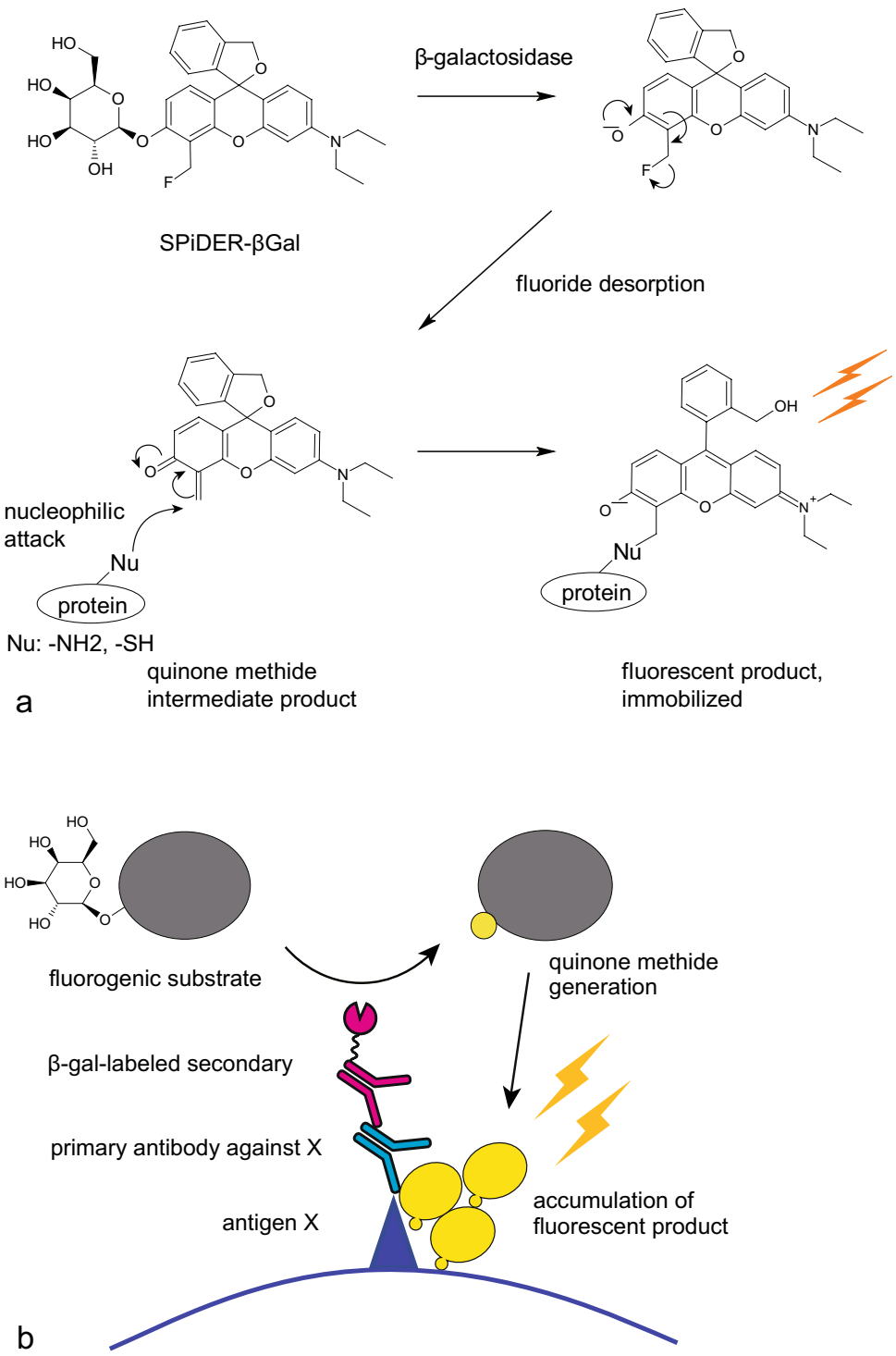

Fig. 1 Catalytic cascade of SPiDER-βGal and the principle of GAFAM staining. SPiDER-βGal is hydrolyzed by β-galactosidase and generates a fluorogenic quinone methide intermediate. The quinone methide reacts with the nucleophile surrounding the reaction site and is covalently immobilized, emitting yellow fluorescence (**a**). The antigen X in the cell or tissue structure is labeled with β-gal by the antigen X and secondary antibodies. The enzyme catalyzes the substrate to the fluorogenic quinone methide. The fluorescence signal is localized on antigen X and amplified, owing to the accumulation of the catalytic product on and near the antigen (**b**)

10×, numerical aperture (N.A.) 0.4, and 20×, N.A. 0.75 (Olympus). The fluorescence filters (Semrock, Lake Forest, IL, USA) are summarized in Table 2. All IF images, except multispectral images, were captured and composited using CellSens Dimension imaging software (version 2.3, Olympus).

Multispectral images were visualized using a Mantra multispectral imaging system with a scientific microscope with a 12-bit multispectral CCD camera [1392 × 1040 pixels] (Akoya Biosciences, Menlo Park, CA, USA) and spectral unmixing was performed using the inForm software, which generated single-color (12-bit grayscale)

Table 1 Antibodies used in this study

Primary antibody against	Clone	Host	Isotype		Dilution	Vendor; product number	RRID
α-SMA	1A4	Mouse	IgG2a		1:400 (0.18 µg/mL)	Agilent (Santa Clara, CA, USA); M0851	AB_2223500
CD45	2B11 + PD7/26	Mouse	IgG1		1:200 (1 µg/mL)	Agilent; M0701	AB_2314143
CK	Polyclonal	Rabbit	IgG		1:200	Agilent; Z0622	AB_2650434
CD31	EP78	Rabbit	IgG		1:100	Cell Marque (Rocklin, CA, USA); 131R-25	AB_2893013
Ki-67	MIB-1	Mouse	IgG1		1:200 (0.23 µg/mL)	Agilent; M7240	AB_2142367
(isotype control)	DAK-GO1	Mouse	IgG1		Same as the primary	Agilent; X0931	AB_2889134
(isotype control)	DAK-GO5	Mouse	IgG2a		Same as the primary	Agilent; X0943	AB_2889133
(isotype control)	Polyclonal	Rabbit	IgG		Same as the primary	Vector Labs. (Burlingame, CA, USA); I-1000	AB_2336355
Secondary antibody against	Clone	Host	Isotype	Label	Dilution	Vendor; product number	RRID
Mouse IgG (H + L)	Polyclonal	Goat	IgG	β-gal	1:500 (2 µg/mL)	Abcam (Cambridge, UK); ab136775	AB_2888623
Rabbit IgG (H + L)	Polyclonal	Goat	IgG	HRP	1:400 (2 µg/mL)	Jackson ImmunoResearch (West Grove, PA, USA); 111-035-144	AB_2307391
Mouse IgG (H + L)	Polyclonal	Goat	IgG	DL405	1:750 (2 µg/mL)	Jackson ImmunoResearch; 115-475-146	AB_2338796
Mouse IgG (H + L)	Polyclonal	Goat	IgG	AF488	1:750 (2 µg/mL)	Jackson ImmunoResearch; 115-545-146	AB_2307324
Mouse IgG (H + L)	Polyclonal	Goat	IgG	AF555	1:1000 (2 µg/mL)	Thermo Fisher (Waltham, MA, USA); A-21424	AB_141780

α-SMA α-smooth muscle actin, *IgG* immunoglobulin G, *CD* cluster of differentiation, *CK* cytokeratin, *β-gal* β-galactosidase from *Escherichia coli*., *HRP* horseradish peroxidase, *DL* DyLight, *AF* Alexa Fluor

Table 2 Fluorescence filters and dichroic mirrors used in this study

Filter set	Excitation wavelength/bandwidth	Emission wavelength/bandwidth	Dichroic cut-off wavelength	Corresponding substrates or fluorochromes
DAPI	350/50 nm	460/50 nm	400 nm	DAPI, MUGF, AMCA, DL405
AQUA	438/24 nm	483/32 nm	458 nm	MUGF3, DEAC
GREEN	494/20 nm	527/20 nm	506 nm	Fluorescein, AF488
GOLD	534/20 nm	572/28 nm	552 nm	SPiDER-βGal
ORANGE	543/22 nm	586/20 nm	562 nm	Cy3, AF555
Cy5	628/40 nm	692/40 nm	660 nm	Cy5

DL DyLight, *AF* Alexa Fluor

and multicolor (merged) images (version 2.46, Akoya Biosciences).

Image analysis and adjustment were performed using Fiji distribution of ImageJ, version 1.53c (https://imagej.nih.gov/ij/). Fluorescence intensity was measured using 14-bit grayscale images. Images were normalized and converted to 8-bit grayscale or 24-bit RGB color for photomicrographs. The brightness and contrast of the images were adjusted using the same conditions for a series of images.

Tissue preparation

Human tonsil and duodenum tissues were obtained as postsurgical specimens at Kyoto University Hospital. This study was conducted after all diagnostic procedures were

completed. Written informed consent was obtained from all patients before tissue collection. The Ethics Committee of Kyoto University Graduate School and Faculty of Medicine approved this study following the Declaration of Helsinki. All tissue samples were anonymized, fixed in 10% neutral-buffered formalin at 25°C for 24 h, and embedded in paraffin. Each FFPE block was cut into 4-μm thick sections, mounted on silane-coated glass slides (Matsunami Glass, Osaka, Japan), and baked at 60°C for 1 h.

General staining procedure

Deparaffinization, heat-induced antigen retrieval (HIAR), and the first iteration of antibody incubation were performed using a BOND-RX automated immunostainer (Leica Biosystems, Wetzlar, Germany). Sample slides were dewaxed using BOND dewax solution (AR9222; Leica Biosystems) at 72°C and then rehydrated using pathology-grade alcohol. HIAR was performed in BOND epitope retrieval solution 2 (AR9640; Leica Biosystems) at 100°C for 20 min. After washing in BOND washing solution (AR9590; Leica Biosystems), the sections were incubated with diluted primary antibody for 60 min, followed by 30 min of incubation with diluted β-gal-, HRP-, or fluorochrome-labeled secondary antibody. The sections were then removed from the immunostainer, immersed in PBS, and subsequent staining was performed manually. Additionally, the appropriate staining controls (isotype-matched immunoglobulins or antibody diluents) were incubated under the same conditions. Fluoromount-G anti-fade (0100-35; Southern Biotechnology, Birmingham, AL, USA) was used as a mountant, unless otherwise stated. The pH of the mountant was approximately 8.5, according to the manufacturer's specifications.

Determination of the optimal staining concentration of β-gal substrates for GAFAM

Serial tonsil sections were incubated with different concentrations of SPiDER-βGal for 30 min. Lymphoid follicles, positive for Ki-67 in each section, were captured under the same conditions. Three Ki-67 positive regions and three Ki-67 negative regions were arbitrarily selected from the respective images of lymphoid follicles, and the fluorescence intensity (gray values) was measured using the ROI Manager of ImageJ. The average gray values per pixel for the three regions were defined as the mean fluorescence intensity (MFI). The optimal concentration of SPiDER-βGal was determined from the MFI of Ki-67-positive regions and the signal to background (S/B) ratio, as well as the image quality of the photomicrographs (e.g., image clarity and signal saturation).

Stability of fluorescence of β-gal substrates

Duodenum sections were stained for anti-α-smooth muscle actin (α-SMA) using MUGF, MUGF3, and SPiDER-βGal (20 μM) according to the general staining procedure, and the fluorescence intensity was measured. After removing the coverslips, the sections were subjected to the denaturation step by heating in citrate–citric acid buffer (CB, 10 mM, pH 6) at 95°C for 20 min using a domestic electric cooker (SR-P37; Panasonic, Osaka, Japan). The sections were then cooled at 25°C for 20 min, followed by imaging. A total of six cycles of the heating–cooling step were repeated in one section, and the respective fluorescence intensity was measured. Subsequently, the background value was subtracted from the fluorescence intensity to calculate the signal intensity relative to the control (i.e., before the first heating step).

Additionally, the signal intensity was evaluated for identical sections mounted with 50% glycerol solutions under different pH conditions of 6, 7.4, and 8.5.

Comparison of sensitivity between β-gal substrates, TSA, and conventional IF

Anti-α-SMA antibodies were used as the primary antibody at different dilutions. HRP-labeled goat anti-mouse immunoglobulin G (IgG) was used for TSA under the same conditions as the β-gal-labeled secondary antibody. For TSA detection, AMCA, DEAC, fluorescein, and Cy3-tyramide were incubated with the sections for 10 min. Additionally, conventional IF stained with DyLight (DL) 405-, Alexa Fluor (AF) 488-, and AF555-labeled goat anti-mouse IgG was compared with those of GAFAM and TSA. After imaging with the corresponding filter sets under the same conditions, the signal intensity of each β-gal substrate was compared with that of fluorochromes with similar wavelength characteristics: AMCA and DL405 for MUGF; DEAC for MUGF3; AF488, fluorescein, and Cy3 for SPiDER-βGal. Chromogenic detection of β-gal was performed using an X-Gal substrate kit (5520-0022; Sera Care, Milford, MA, USA), according to the manufacturer's protocol.

Application of GAFAM to multiplex IF and multispectral imaging

Simultaneous double IF for cluster of differentiation 45 (CD45) and cytokeratin (CK) was performed using a cocktail of primary antibodies on the tonsil sections. Sections were treated according to the general procedure with a secondary antibody cocktail of β-gal-goat anti-mouse and HRP-goat anti-rabbit IgG. CD45 was visualized by GAFAM with SPiDER-βGal, and CK by Cy5-TSA.

Sequential double IF by GAFAM for CD45 and α-SMA was performed on the duodenum sections by repeating the general staining procedure twice. To quench enzyme and antibody activity after the first round, the sections were denatured by heating in CB immediately before the second round at 95°C for 20 min followed by cooling at 25°C for 20 min. CD45 was visualized by SPiDER-βGal and α-SMA by MUGF3. Quadruple IF for α-SMA, CK, CD45, and CD31 was performed by two sequential rounds of simultaneous double IF. As the primary antibody, a cocktail of mouse anti-α-SMA and rabbit anti-CK was used for the first round, and mouse anti-CD45 and rabbit anti-CD31 for the second round. The secondary antibody cocktail was similar to that used for the simultaneous double IF. Heating in CB was performed between the two rounds, as described above. CD45 was visualized by SPiDER-βGal, α-SMA by MUGF3, CD31 by fluorescein-TSA, and CK by Cy3-TSA. Finally, the sections were counterstained with 0.5 μg/mL of 4′,6-diamidino-2-phenylindole dihydrochloride (DAPI, D9542; Sigma-Aldrich). The mounted sections were imaged using a BX63 conventional fluorescence microscope and spectral unmixing was performed using a Mantra multispectral imaging system. A simple flowchart of the GAFAM staining with denaturation step is shown in Fig. 2.

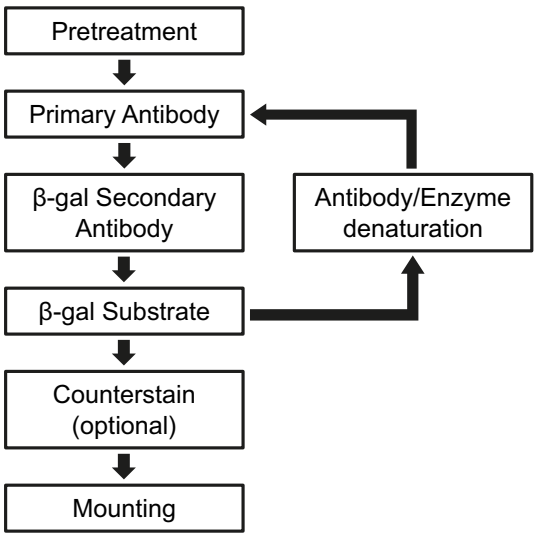

Fig. 2 Flowchart of GAFAM staining procedure. For single staining, the steps in the left column are performed once. For sequential multiple staining, a denaturation step by heating is performed after substrate reaction according to the steps in the right column, and subsequently the steps in the left column are repeated. Multiple staining is possible by repeating this cycle while changing the substrate

Results

The optimal concentration of β-gal substrates

The optimal working concentration of SPiDER-βGal was determined to be representative of β-gal substrates. Ki-67 staining of serial sections of tonsil FFPE tissue was used. Based on the evaluation of the captured images, Ki-67 staining of FFPE tonsil sections by GAFAM with SPiDER-βGal was successful. Ki-67 staining by GAFAM with SPiDER-βGal showed that Ki-67 positivity and morphological clarity in nuclei increased with concentration, and the best

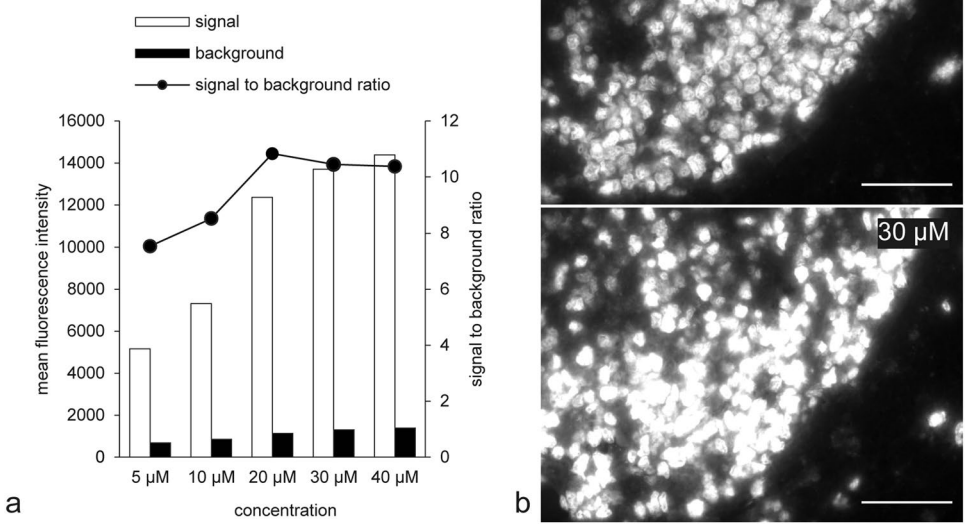

Fig. 3 Optimal conditions for SPiDER-βGal in GAFAM. The bar graph shows the mean signal (white bars) and background (black bars) fluorescence intensity of Ki-67 at different SPiDER-βGal concentrations, and the line chart of the signal-to-background ratio (**a**). Representative Ki-67 images at a SPiDER-βGal concentrations of 20 and 30 μM magnified from Fig. S1 (**b**). Ki-67, as a cell proliferating marker, is positive in many lymphoid cells in the germinal centers of lymphoid follicles. Scale bars: 50 μm

balance was achieved at a concentration of 20 µM (Fig. S1). The MFI of the signal and background (indicated by white and black bars in Fig. 3a) intensified as the concentration of SPiDER-βGal increased. Notably, the S/B ratio increased with concentration and plateaued above 20 µM (line chart in Fig. 3a). The nuclear detail in the image was lost at concentrations above 30 µM owing to signal saturation for the majority of the nuclei (Fig. 3b). Based on these results, 20 µM was selected as the optimal concentration of all β-gal substrates.

Stability of the fluorescence of β-gal substrates

As a cytoplasmic marker, α-SMA was detected in smooth muscle cells, which are mainly present in the blood vessels. The relative signal intensity of MUGF and SPiDER-βGal was maintained at 60%, even after six heating cycles (Fig. 4a, c). The relative fluorescence intensity of MUGF3 was reduced to 60% after the third cycle and to 40% after the sixth cycle (Fig. 4b), although the initial intensity was three to tenfold higher than that of MUGF and SPiDER-βGal, based on exposure time. These results suggest that the three β-gal substrates can be used for mIF with heating.

The fluorescence intensity of all β-gal substrates was reversibly altered in response to variations in pH. The fluorescence intensity of MUGF increased threefold at pH 8.5 compared with that at pH 6 (Fig. 5a). However, the intensity at pH 6 was too low to be distinguished from the background. In contrast, MUGF3 and SPiDER-βGal showed similar stable fluorescence at the three pH values (Fig. 5b, c), but exhibited slightly reduced signals at pH 8.5.

Comparison of the sensitivity between GAFAM, TSA, and conventional IF

The staining sensitivity of β-gal substrates in GAFAM was compared with TSA, conventional IF, and a chromogenic β-gal substrate in the duodenum section (Fig. S2). The fluorescence intensities of MUGF3 and SPiDER-βGal were stronger than that of TSA (Figs. 6c–h), although the intensity of MUGF was weaker than that of AMCA-TSA with the primary antibody at 1:400 (Fig. 6a, b). The fluorescence intensity of conventional IF for AF488 (Fig. 6i; primary antibody dilution 1:400, exposure 350 ms) was similar to SPiDER-βGal with fivefold diluted primary antibody and 1/10 exposure duration (Fig. 6f; primary antibody dilution 1:2000, exposure 35 ms). Therefore, it was concluded that the sensitivity of GAFAM was equal to or greater than that of TSA, which is dozens-fold more sensitive than conventional IF.

Application of GAFAM to mIF in combination with TSA, including multispectral imaging

The expression of CD45 and CK in tissue components is mutually exclusive, because the former is a hematopoietic marker that is mainly expressed on the cell membrane, and the latter is an epithelial marker present in the cytoplasm. During the simultaneous double IF of CD45 and CK, these two markers separated lymphocytes and epithelium in the tonsil (Fig. 7a–c). Similarly, CD45 and SMA, which are expressed in a mutually exclusive manner, were clearly distinguished by sequential double IF (Fig. 7d–g). CD45 signals were localized to the cell membrane and α-SMA to the cytoplasm (Fig. 7g). Fluorescence was clearly detected in the quadruple IF of α-SMA, CK, CD45, and CD31 (Fig. 7h–s). However, spectral cross-talk was observed in the CK and CD45 channels captured by a conventional fluorescence microscope (Fig. 7i, j; see white asterisks). In the merged images from the conventional microscope, the spectral cross-talk of CK (yellow pseudocolor) and CD31 (green pseudocolor) was bright whitish-yellow (mixed color of yellow and green indicated by the white arrows in Fig. 7m). However, spectral cross-talk was not detected in any of the channels generated by spectral unmixing (Fig. 7h–s). These results suggest that the fluorescence wavelength of SPiDER-βGal is similar to that of Cy3 and fluorescein, and the conventional fluorescence microscope could therefore not achieve sufficient separation. Furthermore, multispectral imaging was useful for the application of GAFAM to mIF. In the control experiments, autofluorescence was detected in some channels; however, nonspecific fluorescence originating from the detection system was not observed (Fig. S3).

Discussion

Thus far, no studies have focused on the application of fluorogenic β-gal substrates in IF using FFPE sections. In this study, a novel fluorescence IHC method was developed and evaluated using β-gal as a reporter enzyme, named GAFAM, which was applicable to FFPE samples. GAFAM can be performed in routine procedures (manually or automatically), similar to conventional IF or TSA. It exhibited high sensitivity, comparable to that of TSA, and superior to that of conventional IF. Furthermore, it is suitable for multiplex IF and multispectral imaging.

Three novel fluorogenic β-gal substrates, MUGF, MUGF3, and SPiDER-βGal, were used for GAFAM optimization. The developed protocol indicated that the optimal substrate concentration was 20 µM, and sufficient fluorescence was emitted within 30 min at 25°C. These conditions

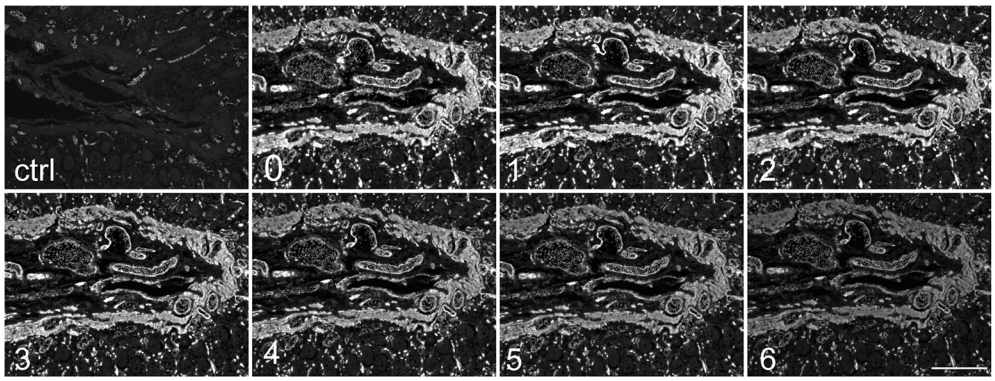

a MUGF

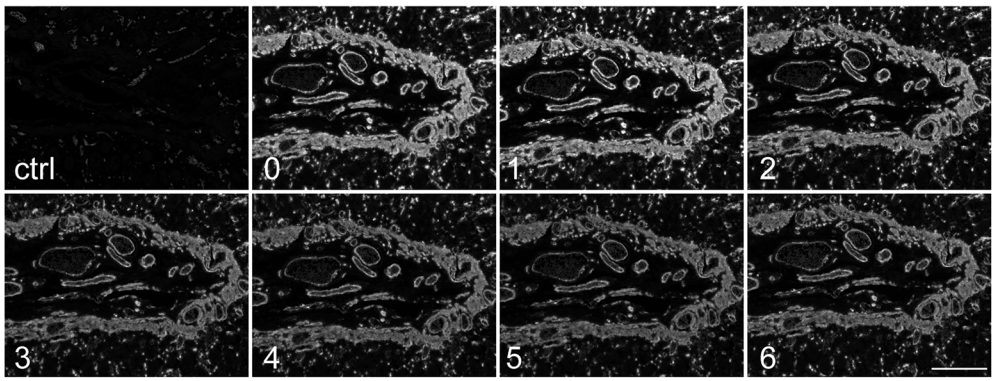

b MUGF3

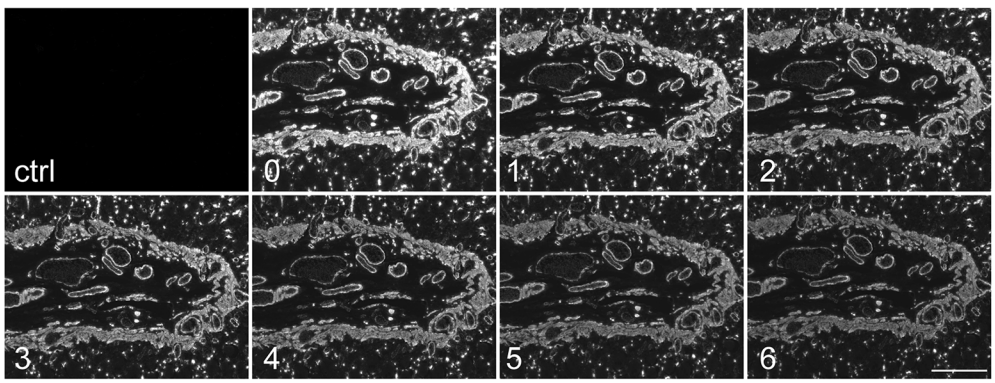

c SPiDER-βGal

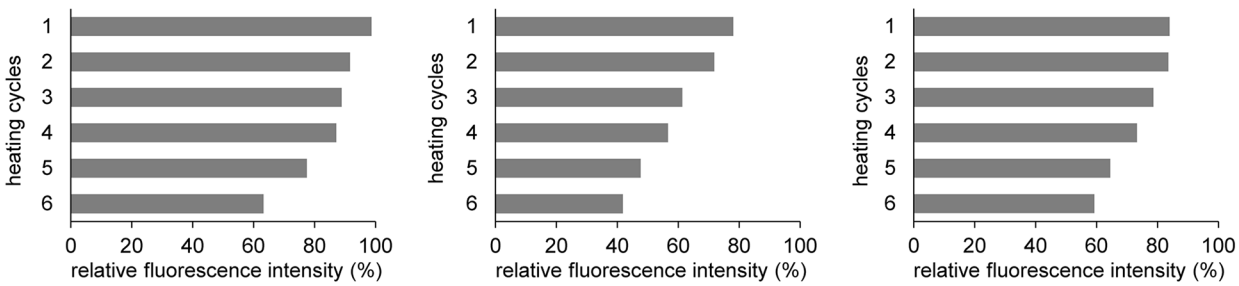

d MUGF MUGF3 SPiDER-βGal

◂**Fig. 4** Stability of the β-gal substrates after repeated heating steps. Photomicrographs of duodenum sections after repeated heating, stained with anti-α-SMA using GAFAM with MUGF (**a**), MUGF3 (**b**), and SPiDER-βGal (**c**). To align the appearance of the initial brightness, the exposure time was adjusted as follows: MUGF for 100 ms, MUGF3 for 10 ms, and SPiDER-βGal for 30 ms. The numeral in each image indicates the number of heating cycles. Each control image is labeled "ctrl." The bar graphs (**d**) show the change in relative signal intensity as a function of the initial brightness (that is, before the first heating step). Scale bars: 200 µm

were suitable for routine staining, which corresponds with previous reports (Doura et al. 2016; Nakamura et al. 2017). The substrate concentration may be further reduced by extending the incubation time or increasing the temperature, similar to other enzyme substrates.

Fluorescence stability after heat denaturation of the antibody and labeling enzyme is essential for mIF. Although various denaturation methods have been reported for multiplexing (Glass et al. 2009; Ikeda et al. 2011; Nakane 1968; van den Brand et al. 2014), heating is the most effective method. The fluorescence quality of the β-gal substrates was assessed after repeated heating–cooling cycles. MUGF and SPiDER-βGal maintained a practical fluorescence intensity after six cycles, indicating the compatibility of mIF staining with TSA. MUGF3 fluorescence was more heat labile than that of the other two compounds. However, MUGF3 could be applied to heat denaturation by adjusting the imaging conditions because its initial brightness was higher than that of the other two β-gal substrates. These results indicated that the three β-gal substrates are theoretically applicable to at least seven-plex mIF.

Fluorochromes containing free hydroxyl groups, such as fluorescein and 7-hydroxycoumarin (umbelliferone), are known for their pH-dependent fluorescence (Fink and Koehler 1970; Martin and Lindqvist 1975). These fluorophores deprotonate to form anions in solution, which are more basic than the pKa value and emit fluorescence. The pKa value of the MUGF fluorescent product was 7.7 (Noguchi et al. 2020). Thus, the MUGF product was presumably deprotonated at pH 8.5 and emitted strong fluorescence (Fig. 5a). However, the signal intensity of MUGF3 and SPiDER-βGal was approximately 20% weaker at a pH of 8.5 than at pH 6 (Fig. 5b, c). Doura et al. described the pH dependence of the SPiDER-βGal absorption and fluorescence spectra. The fluorescence intensity was pH dependent and constant at approximately pH 6–10. Under acidic conditions, a new peak appeared in the short-wavelength region (Doura et al. 2016).Thus, when the fluorescence intensity is sufficiently high, even under acidic conditions, stronger fluorescence may be detected than under alkaline conditions, depending on the characteristics of the applied filter. The fluorescence spectrum of MUGF3 may also change in a similar pH-dependent manner, although the detailed structure has not been clarified thus far. Therefore, the pH of the mountant may have changed the fluorescence intensity of the three β-gal substrates. When the sections stained with β-gal substrates were mounted with Fluoromount-G and maintained at 4°C or −20°C for 1 week, no apparent difference in the fluorescence intensity was observed with storage temperature (data not shown).

GAFAM has the following advantages over TSA and conventional IF: (1) GAFAM has a sensitivity equivalent to TSA and higher than that of conventional IF. Additionally, GAFAM is not time-intensive. Conventional IF generally requires time-consuming protocols (e.g., overnight incubation for primary antibodies), whereas the developed GAFAM protocol is highly sensitive, allowing for shorter antibody incubation and improved results. Consequently, the entire process is completed within a few hours, especially because of the reduced incubation period of primary antibodies. (2) Blue fluorochromes emit fluorescence with a relatively low initial brightness, even second-generation fluorochromes such as DyLight dyes. It is difficult to distinguish the signal of a blue fluorescent probe from tissue components with strong blue autofluorescence, such as collagen and elastin, by conventional IF (Deal et al. 2018). GAFAM using MUGF and MUGF3 is as sensitive as TSA; therefore, it is expected to circumvent the blue fluorescence problem in IF. (3) The lack of quenching of endogenous enzymatic activity is a significant advantage of GAFAM over TSA, because hydrogen peroxide used to quench endogenous peroxidase activity in TSA causes irreversible damage to certain antigenic determinants (Bussolati and Radulescu 2011). Endogenous β-gal activity is negligible in FFPE sections because it is completely inactivated at 58–60°C under standard paraffin embedding conditions (Bondi et al. 1982).

This study aimed to demonstrate that GAFAM could be applied to mIF. Thus, the performance of GAFAM was evaluated compared with mIF using double and quadruple IF. For simultaneous double IHC, primary antibodies derived from two different species and their corresponding secondary antibodies labeled with different enzymes are commonly used to avoid cross-reactions between two targets (van der Loos et al. 1993). This simultaneous staining methodology was applied to GAFAM, and the successful visualization of primary antibodies in mice and rabbits was achieved using GAFAM and TSA, respectively. Subsequently, quadruple IF was achieved by repeating the simultaneous double IF twice. One heating step was required between the two processes to inactivate the antibody and labeling enzyme during the first iteration. Typically, quadruple IF requires three heating steps; however, repeating simultaneous double IF reduces morphological damage and antigenic inactivation caused by frequent heating.

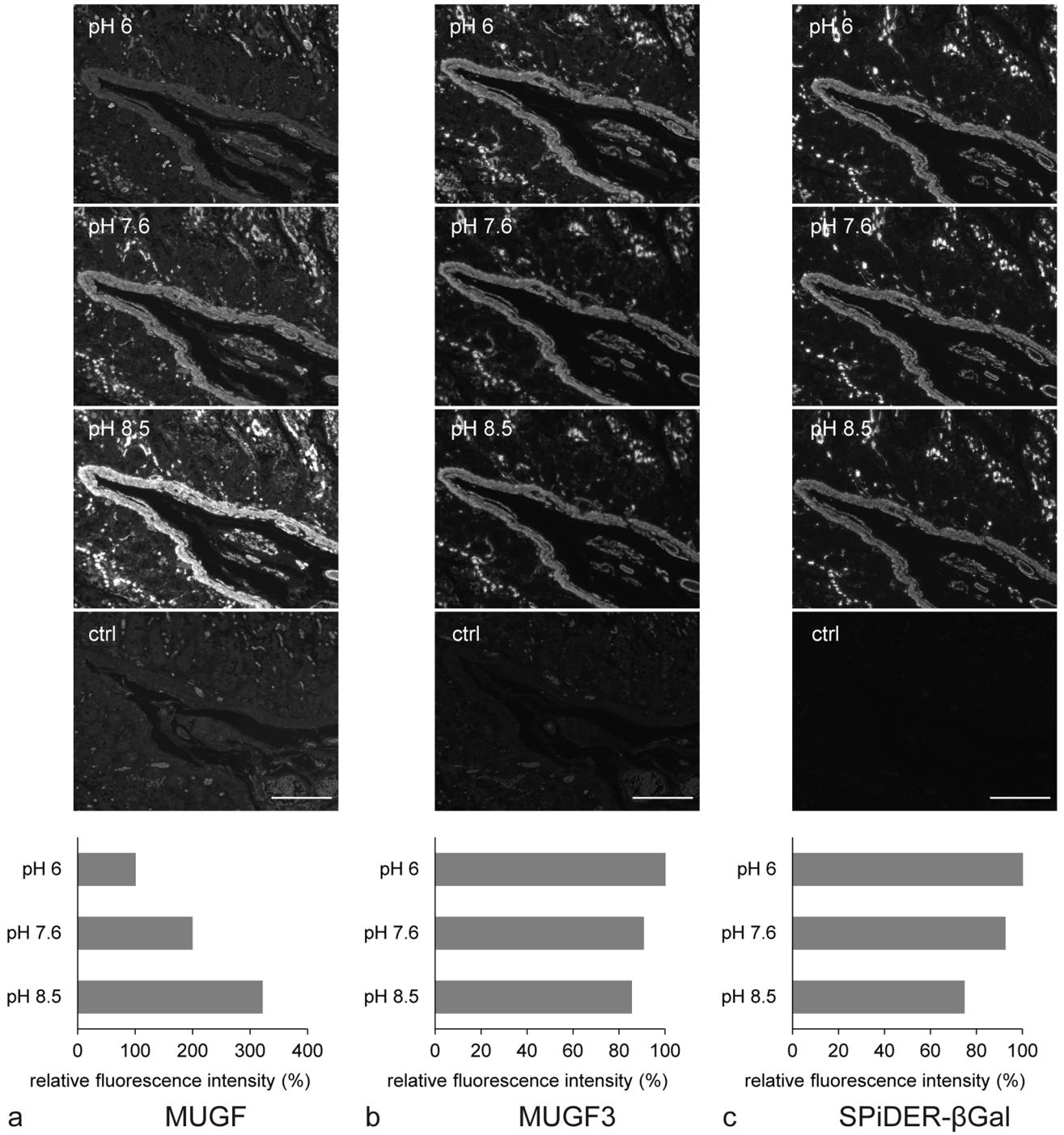

Fig. 5 Signal intensity of GAFAM staining using β-gal substrates under varying pH conditions. Fluorescence intensity of MUGF (**a**), MUGF3 (**b**), and SPiDER-βGal (**c**) evaluated at a pH of 6, 7.4, and 8.5 mountants. Each control image is labeled "ctrl." Bar graphs indicate the relative signal intensity against the pH 6 mountant. Scale bars: 200 µm

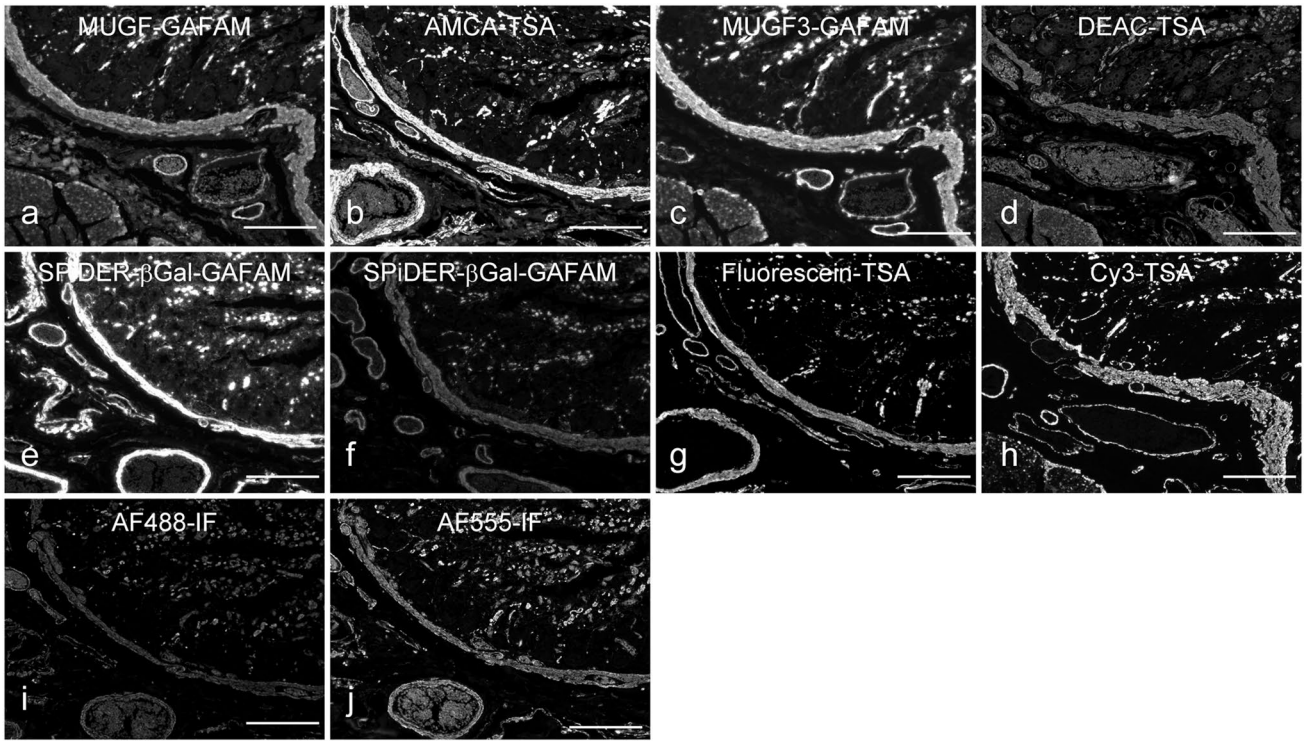

Fig. 6 The sensitivity of GAFAM compared with TSA and conventional IF. The images from GAFAM using MUGF (**a**), MUGF3 (**c**), and SPiDER-βGal (**e**, **f**). The images from TSA using AMCA (**b**), DEAC (**d**), fluorescein (**g**), and Cy3 (**h**). The images from conventional IF labeled with AF488 (**i**) and AF555 (**j**). To compare the sensitivity of fluorophores with a similar spectral profile, each image was captured in the following exposure duration: MUGF, AMCA, and DL405 for 100 ms (**a**, **b**); MUGF3 and DEAC for 20 ms (**c**, **d**); SPiDER-βGal, fluorescein, and Cy3 for 35 ms (**e**–**h**); and AF488 and AF555 for 350 ms (**i**, **j**) to compare with the brightness of images captured by GAFAM and TSA. All images were applied the α-SMA antibody at 1:400 except for image **f** (1:2000), and all β-gal substrates were used at a concentration of 20 µM. Scale bars: 200 µm

GAFAM is a sensitive method that is comparable to current procedures and is a promising tool for biomedical research. However, GAFAM has some limitations. First, its application to a conventional fluorescence microscope is complicated because there are limited fluorescent colors for β-gal substrates. Thus, multispectral imaging was considered. This confirms that unmixing by multispectral imaging is applicable to fluorochromes whose fluorescence spectra do not overlap. However, multispectral imaging did not easily separate MUGF and DAPI, which have identical fluorescence spectra (data not shown). Recently, another β-gal substrate that emits red fluorescence was reported (Ito et al. 2018). Although the substrate has not been tested thus far, it is expected to be applicable to GAFAM. Second, the GAFAM signal is more diffusely localized than the TSA signal. Therefore, GAFAM is suitable for detecting cytoplasmic or extracellular targets such as α-SMA. Polymer compounds suppress the TSA signal diffusion (Van Gijlswijk et al. 1996). Therefore, this method may improve GAFAM signal localization. Third, quinone methide may inhibit other labeling enzymes by reacting with nucleophilic residues in the active enzyme region. During mIHC using different labeling enzymes, the enzyme product inhibits the binding of the antibody to other antigens in the vicinity of the reaction site (known as the "umbrella effect") or reacts with other reaction products to change the color tone (van der Loos 2008; Taube et al. 2020). Thus, the order of enzyme development under prolonged exposure to quinone methide requires further attention. The deposition of quinone methide on proteins is inhibited by nucleophiles; thus, reaction buffers containing Tris base cannot be used.

Overall, GAFAM is a powerful alternative for research using archived FFPE samples. Multiple fluorescent staining is commonly used in various fields, and GAFAM is applicable in the life sciences.

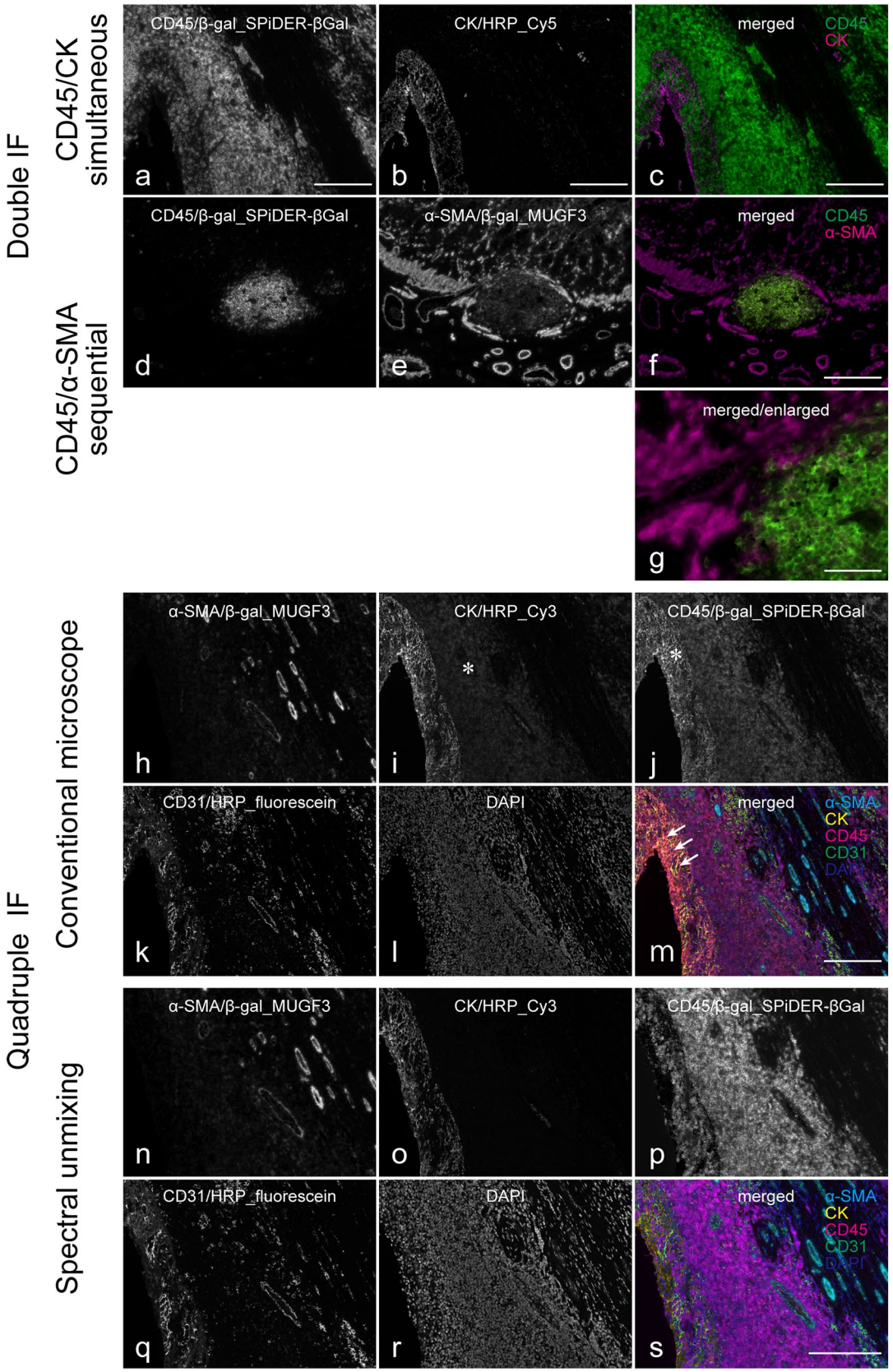
Double IF
CD45/CK simultaneous
CD45/β-gal_SPiDER-βGal
CK/HRP_Cy5
merged
CD45
CK
a
b
c
CD45/α-SMA sequential
CD45/β-gal_SPiDER-βGal
α-SMA/β-gal_MUGF3
merged
CD45
α-SMA
d
e
f
merged/enlarged
g
Quadruple IF
Conventional microscope
α-SMA/β-gal_MUGF3
CK/HRP_Cy3
CD45/β-gal_SPiDER-βGal
h
i
j
CD31/HRP_fluorescein
DAPI
merged
α-SMA
CK
CD45
CD31
DAPI
k
l
m
Spectral unmixing
α-SMA/β-gal_MUGF3
CK/HRP_Cy3
CD45/β-gal_SPiDER-βGal
n
o
p
CD31/HRP_fluorescein
DAPI
merged
α-SMA
CK
CD45
CD31
DAPI
q
r
s

◂**Fig. 7** Double and quadruple IF using GAFAM combined with TSA and application to multispectral imaging. Simultaneous double IF of CD45 and CK (**a**–**c**): grayscale images of CD45-positive lymphocytes labeled with SPiDER-βGal (**a**) and CK-positive epithelial region with Cy5 (**b**); merged image from **a** and **b**, pseudocolored in green and magenta, respectively (**c**). Sequential double IF of CD45 and α-SMA (**d**–**g**): grayscale images of CD45-positive lymphocytes labeled with SPiDER-βGal (**d**) and α-SMA-positive smooth muscle with MUGF3 (**e**); composite image from **d** and **e**, pseudocolored in green and magenta, respectively (**f**). Composite image under high magnification (**g**). Quadruple IF of α-SMA, CK, CD45, and CD31 labeled with MUGF3, Cy3, SPiDER-βGal, and fluorescein, respectively (**h**–**s**): images captured using a BX63 conventional fluorescence microscope (**h**–**m**) and the same area captured and performed spectral unmixing using a Mantra multispectral imaging system (**n**–**s**). Grayscale images of smooth muscle region labeled with α-SMA (**h**, **n**), the epithelial region with CK (**i**, **o**), lymphocytes with CD45 (**j**, **p**), endothelia with CD31 (**k**, **q**), and nuclei with DAPI (**l**, **r**). White asterisks shown in the CK (**i**) and CD45 (**j**) channels indicate spectral overlap. Pseudocolored and merged images (**m**, **s**): in cyan for α-SMA, yellow for CK, magenta for CD45, green for CD31, and blue for DAPI. White arrows shown in **m** indicate the mixed color owing to spectral overlaps of yellow (CK) with green (CD31) channels. Scale bars: 200 μm for entire layout, 50 μm for (**g**)

Supplementary Information The online version contains supplementary material available at https://doi.org/10.1007/s00418-022-02162-5.

Acknowledgements We are grateful to Dr. Takashi Shimomura (Dojindo Laboratories) for kindly providing the chemical compounds MUGF and MUGF3 and for helpful discussions regarding the chemistry of β-gal substrates.

Author contributions Conceptualization: MH; methodology: MH; formal analysis and investigation: MH; writing—original draft preparation: MH and TK; writing—review and editing: all authors; funding acquisition: MH; resources: MH, TK, and HH; supervision: SA and HH.

Funding This work was financially supported by the Policy-Based Medical Services Foundation and Foundation for Promotion of Cancer Research in Japan.

Availability of data and materials The original data presented in this study are available in this article and the supplementary material. Further inquiries can be directed to the corresponding author.

Code availability Not applicable.

Declarations

Conflict of interest The authors have no conflicts of interest to declare.

Ethics approval The Ethics Committee of Kyoto University Graduate School and Faculty of Medicine have approved this study.

Consent to participate Written informed consent was obtained from the patients before sample collection.

Consent to publish Not applicable.

References

Bobrow MN, Harris TD, Shaughnessy KJ, Litt GJ (1989) Catalyzed reporter deposition, a novel method of signal amplification application to immunoassays. J Immunol Methods 125:279–285. https://doi.org/10.1016/0022-1759(89)90104-X

Bondi A, Chieregatti G, Eusebi V et al (1982) The use of b-galactosidase as a tracer in immunocytochemistry. Histochemistry 76:153–158. https://doi.org/10.1007/BF00501918

Bussolati G, Radulescu RT (2011) Blocking endogenous peroxidases in immunohistochemistry: a mandatory, yet also subtle measure. Appl Immunohistochem Mol Morphol 19:484. https://doi.org/10.1097/PAI.0b013e318219a6e6

Cimino-Mathews A (2021) Novel uses of immunohistochemistry in breast pathology: interpretation and pitfalls. Mod Pathol 34:62–77. https://doi.org/10.1038/s41379-020-00697-3

Clutter MR, Heffner GC, Krutzik PO et al (2010) Tyramide signal amplification for analysis of kinase activity by intracellular flow cytometry. Cytom Part A 77:1020–1031. https://doi.org/10.1002/cyto.a.20970

Deal J, Mayes S, Browning C et al (2018) Identifying molecular contributors to autofluorescence of neoplastic and normal colon sections using excitation-scanning hyperspectral imaging. J Biomed Opt 24:1. https://doi.org/10.1117/1.jbo.24.2.021207

Debacq-Chainiaux F, Erusalimsky JD, Campisi J, Toussaint O (2009) Protocols to detect senescence-associated beta-galactosidase (SA-βgal) activity, a biomarker of senescent cells in culture and in vivo. Nat Protoc 4:1798–1806. https://doi.org/10.1038/nprot.2009.191

Dimri GP, Lee X, Basile G et al (1995) A biomarker that identifies senescent human cells in culture and in aging skin in vivo. Proc Natl Acad Sci 92:9363–9367. https://doi.org/10.1073/pnas.92.20.9363

Doura T, Kamiya M, Obata F et al (2016) Detection of LacZ-positive cells in living tissue with single-cell resolution. Angew Chemie 55:9620–9624. https://doi.org/10.1002/ange.201603328

Eyzaguirre E, Haque AK (2008) Application of immunohistochemistry to infections. Arch Pathol Lab Med 132:424–431. https://doi.org/10.5858/2008-132-424-aoiti

Fink DW, Koehler WR (1970) pH Effects on fluorescence of umbelliferone. Anal Chem 42:990–993. https://doi.org/10.1021/ac60291a034

Glass G, Papin JA, Mandell JW (2009) SIMPLE: a sequential immunoperoxidase labeling and erasing method. J Histochem Cytochem 57:899–905. https://doi.org/10.1369/jhc.2009.953612

Hopman AH, Ramaekers FC, Speel EJ (1998) Rapid synthesis of biotin-, digoxigenin-, trinitrophenyl-, and fluorochrome-labeled tyramides and their application for in situ hybridization using CARD amplification. J Histochem Cytochem 46:771–777. https://doi.org/10.1177/002215549804600611

Ikeda K, Suzuki T, Tate G, Mitsuya T (2011) Multiple immunoenzyme labeling using heat treatment combined with the polymer method: an analysis of the appropriate inactivation conditions of primary antibodies. Acta Histochem 113:117–124. https://doi.org/10.1016/j.acthis.2009.08.007

Ito H, Kawamata Y, Kamiya M et al (2018) Red-shifted fluorogenic substrate for detection of lacZ-positive cells in living tissue with single-cell resolution. Angew Chemie Int Ed 57:15702–15706. https://doi.org/10.1002/anie.201808670

Martin MM, Lindqvist L (1975) The pH dependence of fluorescein fluorescence. J Lumin 10:381–390. https://doi.org/10.1016/0022-2313(75)90003-4

Mohler WA, Blau HM (1996) Gene expression and cell fusion analyzed by lacZ complementation in mammalian cells. Proc Natl Acad Sci U S A 93:12423–12427. https://doi.org/10.1073/pnas.93.22.12423

Nakamura Y, Mochida A, Nagaya T et al (2017) A topically-sprayable, activatable fluorescent and retaining probe, SPiDER-βGal for detecting cancer: advantages of anchoring to cellular proteins after activation. Oncotarget 8:39512–39521. https://doi.org/10.18632/oncotarget.17080

Nakane PK (1968) Simultaneous localization of multiple tissue antigens using the peroxidase-labeled antibody method: a study on pituitary glands of the rat. J Histochem Cytochem 16:557–560. https://doi.org/10.1177/16.9.557

Noguchi K, Shimomura T, Ohuchi Y et al (2020) β-Galactosidase-catalyzed fluorescent reporter labeling of living cells for sensitive detection of cell surface antigens. Bioconjug Chem 31:1740–1744. https://doi.org/10.1021/acs.bioconjchem.0c00180

Pratapa A, Doron M, Caicedo JC (2021) Image-based cell phenotyping with deep learning. Curr Opin Chem Biol 65:9–17. https://doi.org/10.1016/j.cbpa.2021.04.001

Price J, Turner D, Cepko C (1987) Lineage analysis in the vertebrate nervous system by retrovirus-mediated gene transfer. Proc Natl Acad Sci 84:156–160. https://doi.org/10.1073/pnas.84.1.156

Speel EJM, Ramaekers FCS, Hopman AHN (1997) Sensitive multicolor fluorescence in situ hybridization using catalyzed reporter deposition (CARD) amplification. J Histochem Cytochem 45:1439–1446. https://doi.org/10.1177/002215549704501013

Stack EC, Wang C, Roman KA, Hoyt CC (2014) Multiplexed immunohistochemistry, imaging, and quantitation: a review, with an assessment of tyramide signal amplification, multispectral imaging and multiplex analysis. Methods 70:46–58. https://doi.org/10.1016/j.ymeth.2014.08.016

Sugizaki T, Zhu S, Guo G et al (2017) Treatment of diabetic mice with the SGLT2 inhibitor TA-1887 antagonizes diabetic cachexia and decreases mortality. NPJ Aging Mech Dis 3:12. https://doi.org/10.1038/s41514-017-0012-0

Sukswai N, Khoury JD (2019) Immunohistochemistry innovations for diagnosis and tissue-based biomarker detection. Curr Hematol Malig Rep 14:368–375. https://doi.org/10.1007/s11899-019-00533-9

Tan WCC, Nerurkar SN, Cai HY et al (2020) Overview of multiplex immunohistochemistry/immunofluorescence techniques in the era of cancer immunotherapy. Cancer Commun 40:135–153. https://doi.org/10.1002/cac2.12023

Taube JM, Akturk G, Angelo M et al (2020) The society for immunotherapy in cancer statement on best practices for multiplex immunohistochemistry (IHC) and immunofluorescence (IF) staining and validation. J Immunother Cancer. https://doi.org/10.1136/jitc-2019-000155

Teixidó C, Vilariño N, Reyes R, Reguart N (2018) PD-L1 expression testing in non-small cell lung cancer. Ther Adv Med Oncol 10:1–17. https://doi.org/10.1177/1758835918763493

van den Brand M, Hoevenaars BM, Sigmans JHM et al (2014) Sequential immunohistochemistry: a promising new tool for the pathology laboratory. Histopathology. https://doi.org/10.1111/his.12446

van der Loos CM (2008) Multiple immunoenzyme staining: methods and visualizations for the observation with spectral imaging. J Histochem Cytochem 56:313–328. https://doi.org/10.1369/jhc.2007.950170

van der Loos CM (2010) Chromogens in multiple immunohistochemical staining used for visual assessment and spectral imaging: the colorful future. J Histotechnol 33:31–40. https://doi.org/10.1179/his.2010.33.1.31

van der Loos CM, Becker AE, van den Oord JJ (1993) Practical suggestions for successful immunoenzyme double-staining experiments. Histochem J 25:1–13. https://doi.org/10.1007/BF00161039

Van Gijlswijk RPM, Wiegant J, Raap AK, Tanke HJ (1996) Improved localization of fluorescent tyramides for fluorescence in situ hybridization using dextran sulfate and polyvinyl alcohol. J Histochem Cytochem 44:389–392. https://doi.org/10.1177/44.4.8601698

Viratham Pulsawatdi A, Craig SG, Bingham V et al (2020) A robust multiplex immunofluorescence and digital pathology workflow for the characterisation of the tumour immune microenvironment. Mol Oncol 14:2384–2402. https://doi.org/10.1002/1878-0261.12764

Supplementary Information

Supplementary Fig. S1 Ki-67 staining by GAFAM at different concentrations of SPiDER-βGal. Scale bars: 50 μm

Supplementary Fig. S2 The sensitivity of GAFAM compared with TSA and conventional IF. Each row indicates the substrates for GAFAM and conjugated tyramides for TSA. The conventional IF and X-gal chromogenic detection are shown in the bottom row. The dilution factor of the primary antibody is indicated under each lane. Parts of this figure were presented in Fig. 6. Scale bars: 200 μm

Supplementary Fig. S3 Control study for double and quadruple IF using GAFAM combined with TSA. Each panel shows simultaneous double IF of CD45/CK (a), sequential double IF of CD45/α-SMA (b), quadruple IF of α-SMA/CK/CD45/CD31 under the BX63 conventional fluorescence microscope (c), and the same quadruple IF as (b) under the Mantra multispectral imaging system (d). The primary antibody is shown in the upper row in each panel, and the corresponding isotype-matched controls are shown in the lower row. Parts of this figure are presented in Fig. 7. Scale bars: 200 μm

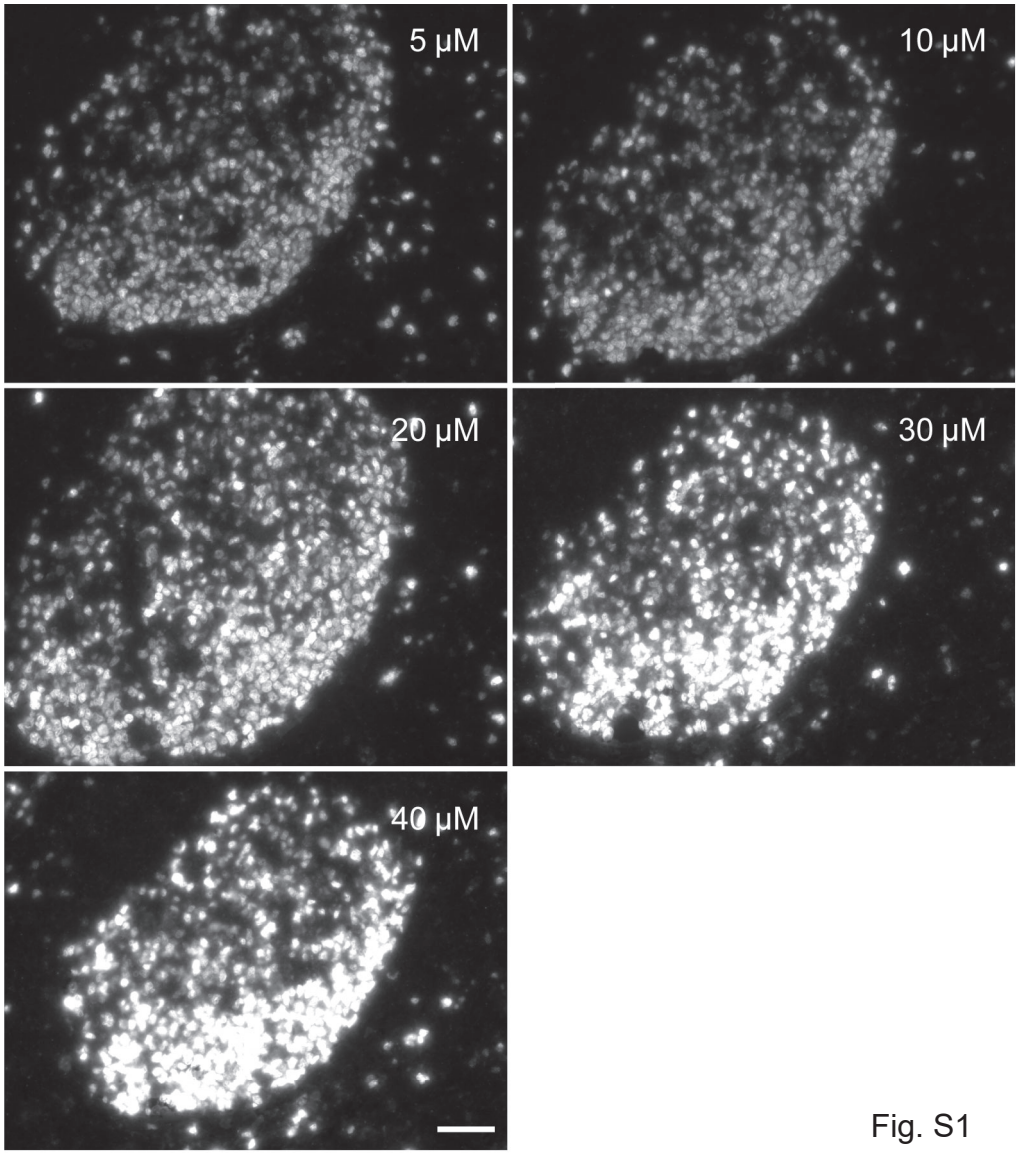

Fig. S1

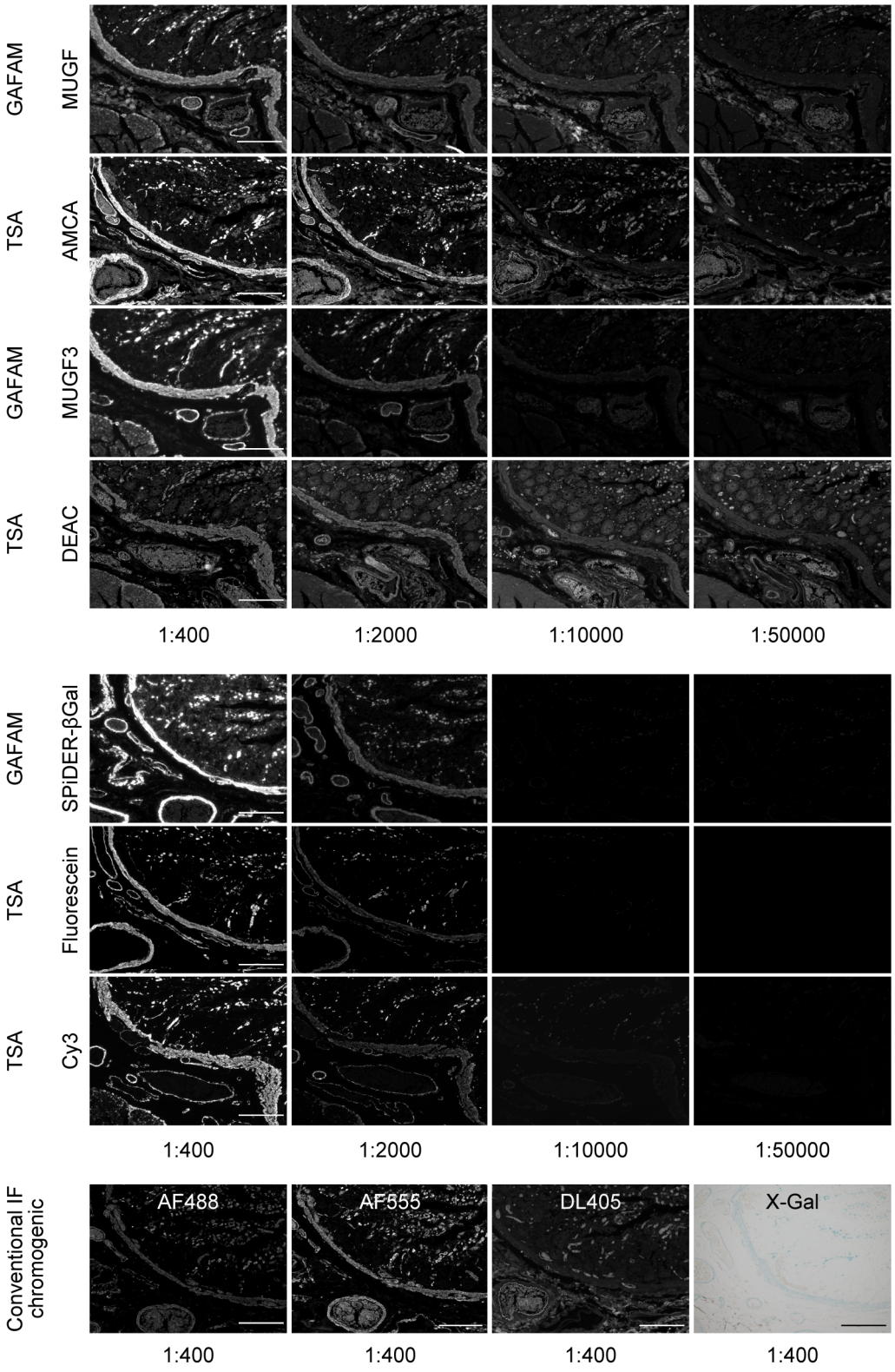
GAFAM
MUGF
TSA
AMCA
GAFAM
MUGF3
TSA
DEAC
1:400
1:2000
1:10000
1:50000
GAFAM
SPiDER-βGal
TSA
Fluorescein
TSA
Cy3
1:400
1:2000
1:10000
1:50000
Conventional IF chromogenic
AF488
AF555
DL405
X-Gal
1:400
1:400
1:400
1:400

Fig. S2

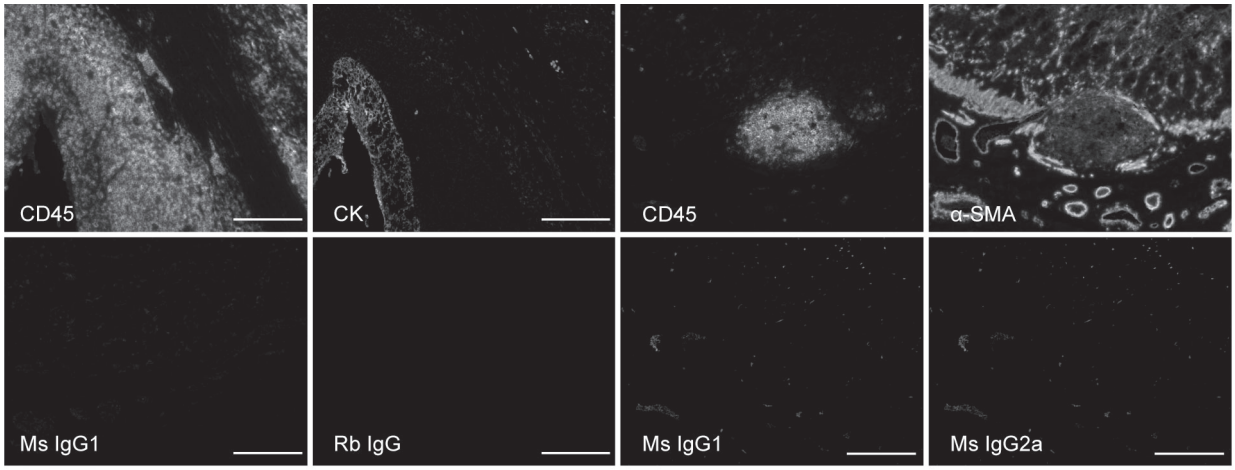

a CD45/CK simultaneous b CD45/α-SMA sequential

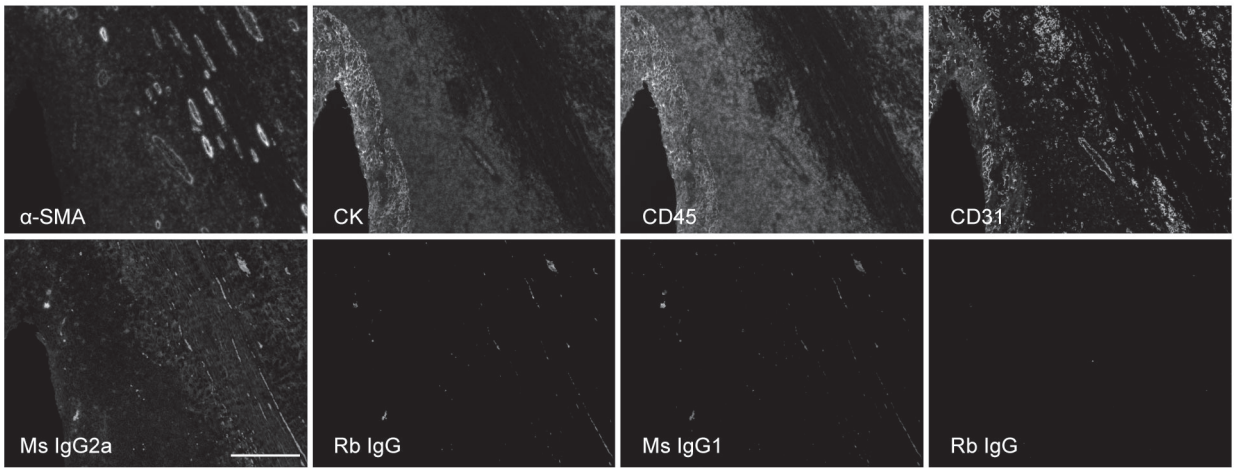

c α-SMA/CK/CD45/CD31_conventional

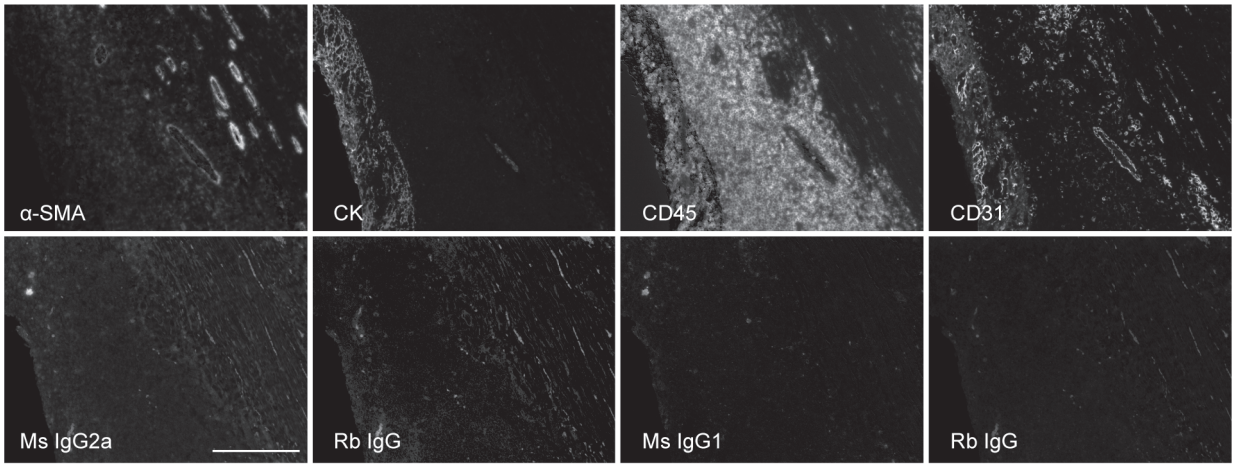

d α-SMA/CK/CD45/CD31_multispectral

Fig. S3